Fast cure of stable semi-pregs via VBO cure

David B. Bender , Timotei Centea & Steven Nutt

Published online: 05 Jan 2021.

Submit your article to this journal ⬀

View related articles ⬀

View Crossmark data ⬀

Taylor & Francis
Taylor & Francis Group

OPEN ACCESS

Check for updates

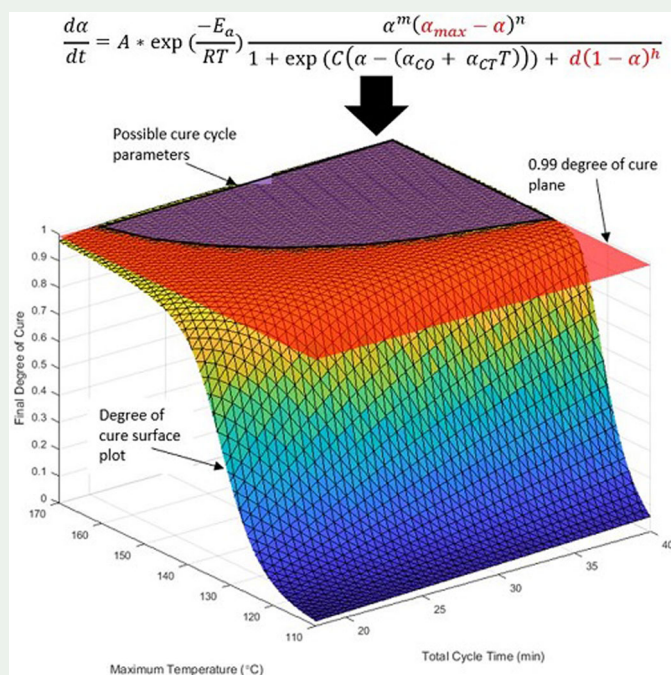# Fast cure of stable semi-pregs via VBO cure

David B. Bender ⬤, Timotei Centea and Steven Nutt ⬤

M.C. Gill Composites Center, Viterbi School of Engineering, University of Southern California, Los Angeles, CA, USA

ABSTRACT

To address the need for increased efficiency in high performance composite processing, a vacuum bag only (VBO) semi-preg was designed, modeled, and evaluated. The semi-preg featured a vinyl hybrid resin formulated for rapid cure. A model was developed to describe the kinetic behavior of the resin, and then was employed to guide the design of efficient cure cycles. The semi-preg featured a discontinuous distribution of resin on the fiber bed. The format imparted high through-thickness air permeability by virtue of the multitude of air evacuation pathways with short breath-out distances relative to conventional out-of-auto-clave prepregs (OoA). The kinetic model was used to create a test matrix of panels from the semi-pregs. Microstructural quality, interlaminar shear strength, and glass transition temperature were compared to a control panel with a longer, conventional cure cycle. The results demonstrated that fast-cure resins can be used in conjunction with cure modeling and semi-preg formats to design appropriate VBO cure cycles that consistently yield parts with low defect contents without autoclaves.

GRAPHICAL ABSTRACT

$$\frac{d\alpha}{dt} = A * \exp\left(\frac{-E_a}{RT}\right) \frac{\alpha^m (\alpha_{max} - \alpha)^n}{1 + \exp\left(C\left(\alpha - (\alpha_{CO} + \alpha_{CT}T)\right)\right) + d(1-\alpha)^h}$$

1. Introduction

The objectives of the present work were to modify standard cure models to accurately predict cure kinetics of a fast cure resin for prepregs that allow for fast cure cycles (minutes) through rapid air removal in vacuum bag only (VBO) processing and to explore cure cycle modifications to reduce cycle times. The new model was developed to describe the kinetic behavior of the fast-curing resin, because conventional models do not accurately predict the cure behavior. A discontinuous pattern of resin was deposited on a woven fiber bed to produce semi-pregs. The resulting semi-pregs then were used to fabricate panels, which were evaluated for quality and performance.

CONTACT David B. Bender ✉ dbender@usc.edu 🖥 M.C. Gill Composites Center, Viterbi School of Engineering, University of Southern California, 3651 Watt Way, VHE-402, Los Angeles 90089 CA, USA

The production rate of high-performance composites is presently limited by lengthy cycle times and costly, labor-intensive manufacturing processes that require curing in autoclaves. VBO processing of prepregs can mitigate these limitations, particularly the need for autoclaves, but VBO processing sacrifices process robustness, requires long cycle times (hours), and frequently requires protracted debulking (vacuum holds). These limitations stem largely from both the resin chemistry and the conventional design of VBO prepregs, which rely on edge-breathing for air removal [1]. Nevertheless, the use of out-of-autoclave (OoA) processes continues to grow, driven by the need to reduce both the process cycle time and the manufacturing cost of composite laminates. Doing both will reduce barriers to entry and expand the use of these high-performance materials.

1.1. Background

In the aerospace industry, production of composite parts from prepregs generally involves curing in autoclaves, primarily to limit porosity and to yield consistency in part quality. Voids within composite materials reduce mechanical performance, generating stress concentrations that lead to premature failure. Consequently, parts with porosity levels >1% are generally rejected [2]. Autoclaves apply pressure (and temperature) on the laminates during cure that suppress volatile evolution from the resin [3]. Thus, autoclave processing consistently yields void-free parts. However, capital and operating costs are high relative to ovens, and throughput is severely restricted, both by the autoclave and by the kinetics of cure in conventional thermoset prepregs [4]. The lengthy startup time and intensive resource consumption of autoclaves make it difficult to increase production efficiency, and prevent in-field processing often required for repairs and modifications [5]. These issues provide the impetus for development of out-of-autoclave (OoA)/vacuum bag only (VBO) prepregs, which are designed to be cured in conventional ovens [6].

The key to VBO processing of prepregs lies in control of porosity [7]. Without super-ambient pressure to suppress void development, extra care must be taken to ensure complete removal of air and/or evolved gases from the prepreg while it is being cured. The design of conventional VBO prepregs features partially impregnated resin on both sides of the fiber bed, creating a dry channel in the ply mid-plane that allows gases to egress via edge-breathing dams [8]. Air trapped between and within plies, as well as evolved volatiles, must be evacuated before the resin fully saturates the fiber bed and gels [9]. However, gases that are not completely removed remain as voids after gelation. Thus, imperfect or adverse conditions during cure of edge-breathing VBO prepreg can result in porosity levels >1%. Because of this, VBO prepreg plies must undergo "debulking" (extended vacuum hold) to remove air prior to cure [10]. Although the setup time for ovens or heat blankets is less than that of autoclaves, debulking can often render VBO processing more time consuming than autoclave cure, particularly for large or complex parts. Thus, VBO processing does not always reduce cycling times.

Compounding the challenges above, scenarios arise where gas evacuation via edge-breathing is not feasible. One such example is the co-cure of composite repair patches [11]. Because patches are inserted into fully cured parent material, the pathways for gas egress via edge-breathing are generally blocked. The situation is further complicated by adhesive layers, which ensure strong bonding but prevent air egress. Although methods are available to mitigate these problems (such as double vacuum debulking (DVD)), they are difficult to implement and do not ensure void-free parts [12]. Because of the difficulty of these methods, hard patches cured in autoclaves are often employed instead of co-cured patches, despite often being weaker and less versatile [13]. With VBO prepregs, whether in a manufacturing environment or an in-field repair, these issues are exacerbated in larger and thicker parts. When manufacturers consider substituting composites for conventional materials, they are deterred by the large capital investments required, or by lack of robustness of VBO processing. In both autoclave and VBO methods, making a single part requires hours of processing.

Epoxies are widely used resins in the aerospace industry, and the cure kinetics are well-characterized [14]. Cure cycles for VBO epoxy prepregs often last several hours. After debulking, these cure cycles typically include an intermediate temperature dwell to allow resin to flow and fully impregnate the composite. This stage is followed by a high-temperature dwell to fully cure the laminate. The cure kinetics of the epoxy employed dictate the duration of the cure step. Epoxy cure releases heat (exotherm), and thus ramp rates are limited to mitigate the risk of damage from overheating [15]. These factors contribute to longer cure cycles. Although the aerospace industry employs such cycle times, the automotive industry requires much faster cure cycles to achieve high production rates [16]. While performance requirements for automotive structures are less demanding than aerospace materials, composites capable of being employed in these and other industries often require cure cycles of minutes as opposed to hours [17].
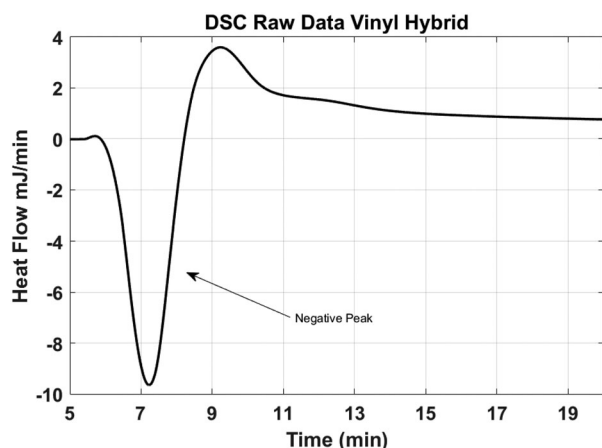
Figure 1. DSC raw data for isothermal hold at 140 °C showing the negative peak.

Deployment of prepregs in industries with high production volumes may require resins formulated for fast cure cycles, as well as prepregs suited to VBO curing. Fast curing requires an alternate cure chemistry distinct from conventional resins, such as epoxies. To avoid autoclave cure, such resins must be coupled with a prepreg format that does not rely on edge breathing for gas removal. Although porosity less than 1% may not be required for applications outside of aerospace, void contents exceeding 4% are undesirable [18]. Addressing both issues of cure kinetics and porosity is critical for widespread adoption of prepregs in industries requiring rapid production rates.

As thermoset resins employed in composites continue to become more complex, modeling their behavior has required additional terms to be included. The model described by Kamal *et al* employed autocatalytic terms to model a single epoxy cure reaction [19]. It used the assumption that cure rate can be given by current degree of cure and temperature combined with the Arrhenius dependence on autocatalytic polymerizations to model thermoset behavior. When diffusion limitations were found to impact cure rates, a model described by Cole *et al* was developed to account for those effects [20]. To describe fast curing resin behavior with diffusion limitations, Grindling included additional terms to account for chemical-controlled states (in addition to diffusion-controlled states) [21]. With fast curing, room temperature stable resins now being employed, a new model to account for those features is needed.

This study addresses the limitations of conventional kinetic models to describe novel fast curing thermoset resin behavior with room temperature stability. Current thermoset models are unable to account for room temperature stability and its effect on cure behavior. The effect of prepreg formatting on potential cycle time reduction without adversely affecting porosity levels was explored. Previous work

on semi-pregs used resins without fast curing or other unusual kinetic behaviors [22]. The pairing of fast-curing resin on a formatted prepreg represents a new design space for VBO materials.

In this study, a fast-curing resin was used to produce prepreg with high through-thickness permeability (semi-preg). New terms are introduced to a conventional autocatalytic model to describe the unusual kinetic behavior of the resin. The model is employed to design fast-cure cycles that are processed with a single vacuum bag, delineating how cure cycle features (debulk time, intermediate hold time, final temperature) affect the quality and performance of cured laminates. Using the model, fully cured panels with <4% porosity are fabricated with cure cycles of less than an hour.

2. Experiments

A fast-cure vinyl hybrid resin with characteristics suitable for the present study was selected [23]. The resin, originally designed for resin infusion, featured a vinyl ester base but differed from conventional vinyl esters in that styrene was not required to form crosslinks. The absence of styrene reduced volatiles normally released during cure and decreased void evolution. The reduced release of volatiles was confirmed by thermogravimetric analysis (TGA, TA Instruments Q5000).

The vinyl hybrid resin relies on an unusual cure chemistry that features reaction inhibition before the cure temperature is reached. The inhibition allows the resin to remain at low viscosity prior to gelation and imparts room temperature stability, obviating the need for cold storage. Room temperature stability thus imparts cost savings and convenience, particularly for applications such as in-field repair. The rapid cure kinetics of the resin requires modification to conventional cure kinetics models, as described in the modeling section.

The vinyl hybrid reaction kinetics were analyzed using dynamic scanning calorimetry (DSC, TA Instruments Q2000), to measure heat flow data as a function of time and temperature. Neat resin samples (10 mg) were employed. Test conditions included five dynamic ramps (1–10 °C/min) up to 200 °C and twelve isothermal holds (93–163 °C). Because of the rapid cure reaction, the instrument did not capture the entirety of the exotherm during isothermal holds. The result was a negative peak that resulted from supplying heat to the pan while the resin underwent the exotherm. The negative peak from instrument heating was thus convoluted with the peak from the exotherm. An example of the phenomenon exhibited in a 140 °C is shown in Figure 1.

To address the "negative peak" phenomenon, additional steps were taken to compensate and to retain the information needed to generate an accurate cure model. First, the total heat of reaction was measured for all the ramp runs, and the average was then used as the baseline. At the end of every isothermal run, a ramp test was immediately performed on the isothermal sample to measure the remaining heat yet to be released. The excess heat released from the ramp run was subtracted from the total heat of reaction, yielding the heat released from the isothermal run.

Code was written in Visual Basic and used to analyze the raw data from the isothermal runs. The code was used to generate a linear baseline and to perform degree of cure calculations, eliminating human error in the process and allowing comparative analysis. The heat released (determined from the code) was used to determine the resin degree-of-cure after the negative peak phenomenon. Thus, experiments frequently yielded plots of degree-of-cure versus time that were offset from zero degree-of-cure (see for example, Figure 3). Once the isothermal tests could be accurately adapted and included, the results from both isothermal and dynamic experiments were incorporated into the modeling analysis.
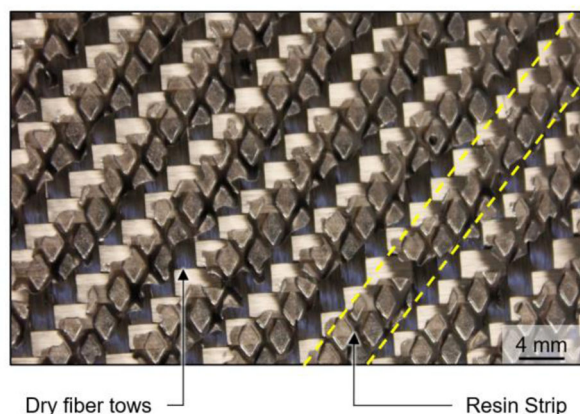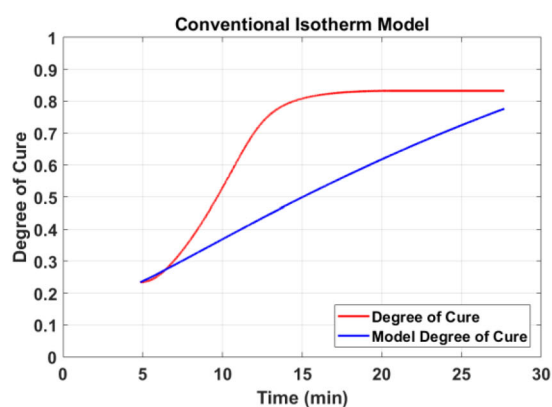
The resin was applied to carbon fiber fabric to produce semi-preg, an unconventional prepreg format that features discontinuous distributions of resin [24]. The discontinuous resin facilitates rapid air removal by imparting permeability in the through-thickness direction. Conventional prepregs rely solely on in-plane air evacuation pathways *via* ply edges, but semi-preg introduces an abundance of much shorter pathways for gas egress. In addition, challenges that arise when executing in-field repairs become manageable. One embodiment of semi-preg showing dry fiber tows and resin strips is shown in Figure 2.

Semi-pregs comprised of 2×2-twill carbon fabric with 6 K tows (Dow Aksa A-38) and identical layup procedures were used for all panels. Non-perforated fluorinated ethylene propylene (FEP) release film (Airtech A4000) was taped to an aluminum tool plate, 450×450 mm. A thin tool plate was chosen to minimize the heat sink effects of a thicker plate. The prepreg measuring 150×150 mm was then laid up in a quasi-isotropic stacking sequence of $[0°/45°]_{2s}$ with 8 plies for each panel.

The panel edges were sealed using sealant tape. The sealant tape dams prevented edge breathing that would normally reduce debulking time, but more importantly, sealed edges demonstrated the efficacy of the semi-preg format for air evacuation. Sealing edges also eliminated concerns of resin bleed. To complete the vacuum bagging, the laminate was covered with a layer of perforated FEP release film. The perforations were spaced every 50 mm to limit resin bleed from the low-viscosity resin.

A layer of nylon breather cloth (Airtech Airweave N10) was placed atop the perforated FEP layer. The vacuum bag was then sealed and placed in an insulated chamber. The bag was then covered with a heat blanket. The insulation reduced heat losses to the environment, allowing rapid and more accurate temperature control. Heat blanket temperature was controlled using K-type thermocouples and a
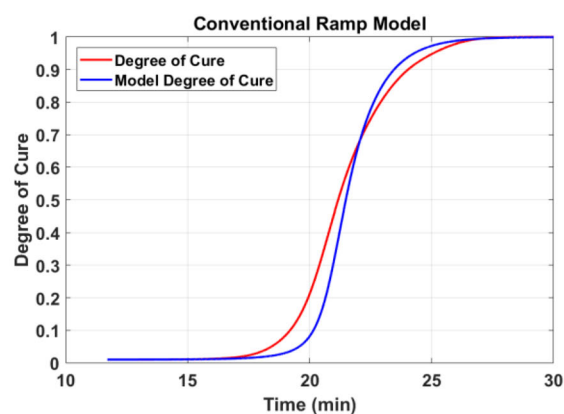

Dry fiber tows ⌐   Resin Strip

Figure 2. Semi-preg format.

Figure 3. Modeling with conventional equation - **a)** Isothermal test at 116 °C, and **b)** Ramp test at 2 °C/min.

controller (Watlow PM6R1CA-AAAAAAA). The laminate temperature was measured using K-type thermocouples centrally located on the bagging film. Vacuum was applied with a dedicated vacuum pump (Busch R5). Bag pressure was monitored using a gauge on the bag, and a vacuum level of >96.5 kPa was maintained throughout the cure cycle. Cure cycles were designed after DSC data was analyzed and modeled.

Glass transition temperature was determined using dynamic mechanical analysis (DMA, TA Instruments Q800). Samples measuring 60×12 mm were cut from the panels and tested with dual cantilever mode using a test frequency of 1 Hz and a drive force of 18 N. The samples were heated at 3 °C/min beyond the glass transition temperature. The T_g was identified as the peak of the tangent delta curve.

Porosity was measured from polished sections, 25 mm. Cross sections were ground and polished to 4000 grit. Images were acquired using a digital stereo microscope (Keyence VHX 600) at $200\times$ magnification. Void content was calculated by measuring the ratio of void area to the total prescribed area for each polished sample. Void areas were indicated using a combination of binary thresholding and manual input.

Interlaminar shear strength was measured according to ASTM 2344 D. Samples, having a width of two times the thickness and a span greater than six times the thickness, were prepared. Samples were loaded at a rate of 1 mm/min until failure. The maximum load was used to calculate short beam shear strength.

3. Results

3.1. Modeling

The data from the DSC was first inserted into the widely-used kinetic model from Khoun et al [25].

$$\frac{d\alpha}{dt} = A * \exp\left(\frac{-E_a}{RT}\right) \frac{\alpha^m(1-\alpha)^n}{1 + \exp\left(C(\alpha - (\alpha_{CO} + \alpha_{CT}T))\right)} \tag{1}$$

The expression describes autocatalytic cure with a rate-limiting diffusion factor. Using this equation, multivariable minimization of error was applied to determine values for the terms. The error was minimized across 17 isothermal and ramp DSC runs. However, systematic discrepancies appeared between the cure data and values predicted from the model. The discrepancies were especially apparent in isothermal DSC runs (Figure 3a).

Despite efforts to determine terms that yielded a closer match, significant differences remained

between measured and model predictions. Also, in some isothermal runs, the resin did not reach full cure. The conventional model had no way of accounting for this phenomenon to this extent, and adjustments were required. For dynamic (ramp) tests, data sets correlated more closely, yet still exhibited systematic discrepancies (Figure 3b).

For dynamic heating, the model predictions consistently lagged behind the measured data, indicating delayed cure in early stages (up to $\alpha = 0.7$). The delayed cure kinetics was consistent with the room temperature stability of the vinyl hybrid. The measured cure rate also decelerated more quickly than the model cure rate as full cure was approached. The observed rapid deceleration in reaction rate indicated that the rate-limiting diffusion terms were more influential than the model was predicting. However, the diffusion terms were not accurately represented in the conventional model, because an important aspect of the vinyl hybrid resin was not considered. The room temperature stability of vinyl hybrid required a modified cure cycle that took this characteristic into account. Therefore, a phenomenological model (fast-cure, or FC model) was formulated to account for the inhibition. The new expression includes a term to account for inhibition, as well as a term to account for incomplete cure at lower temperatures.

$$\frac{d\alpha}{dt} = A * \exp\left(\frac{-E_a}{RT}\right)$$
$$\frac{\alpha^m(\alpha_{max} - \alpha)^n}{1 + \exp\left(C(\alpha - (\alpha_{CO} + \alpha_{CT}T))\right) + d(1-\alpha)^h} \tag{2}$$

In this expression, the cure rate is represented as a function of α and temperature. In the numerator, the term $(\alpha_{max} - \alpha)$ is used instead of $(1 - \alpha)$ to account for the resin not fully curing at lower temperatures. Although α_{max} in most cases will be 1, the distinction is necessary for accurate modeling of the rapid cure kinetics, a feature manifest in the isothermal measurements.

In the denominator, the term with d and h accounts for cure inhibition at lower temperatures. This new term allows the degree of cure to remain near zero until a threshold α is reached, after which the autocatalytic terms dominate. Inclusion of the new term altered the values for other terms in the expression. For example, the activation energy E_a, and autocatalytic terms n and m, were decreased in the new expression relative to the conventional (Khoun) model. The model (using the values, $A = 4.86e7 \ s^{-1}$, $E_a = 5.02e4$ J/mol, $m = 0.39$, $n = 0.21$, $C = 1.08$, $\alpha_{Co} = -55.0$, $\alpha_{CT} = 0.12 \ K^{-1}$, $d = 1830$, and $h = -1.43$), represents fast cure kinetics more
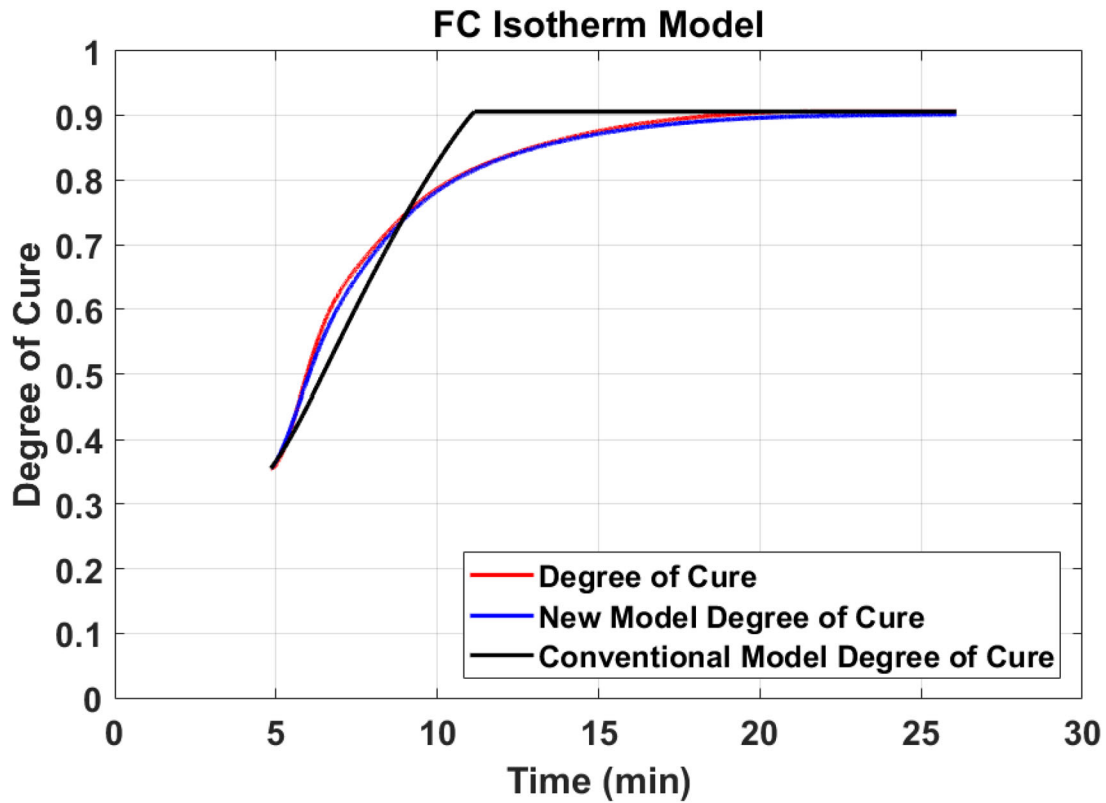
Figure 4. Isothermal cure showing predictions of fast-cure model and conventional model.

accurately than the Khoun model. In the denominator, the effect of the diffusion term became more pronounced, and the C term decreased, while α_{Co} and α_{CT} both increased relative to the Khoun model.

When the FC model predictions were plotted alongside measured results, the data sets were more closely aligned, especially for the isotherm tests. The percent deviation between predictions of the revised model and measured data was <5%, with negligible variance (Figure 4). In contrast, the percent deviation for the conventional (Khoun) model degree of cure on isothermal tests was often >30% and exhibited variability.

When dynamic heating runs were inserted into the FC model, the results did not display the systematic discrepancies described above. The FC model accounted for cure inhibition, and thus more accurately simulated early stages of cure. The altered diffusion terms eliminated the lag predicted by the conventional (Khoun) model.

The final degree of cure α_{max} does not always reach $\alpha_{max} = 1$ (shown in isothermal data). Thus, an expression for α_{max} as a function of the maximum temperature is required for the FC model, and this expression must also include the threshold curing temperature. One such model for α_{max} is:

$$\alpha_{max} = 1 - \frac{1}{1 + k * \exp(q * (T_{max} - T_c))}$$

where the constants k and q were determined using minimization of error. The term T_C represents the temperature at which the cure reaction commences

(105 °C, from DSC results). The value determined from DSC measurements was compared with a separate minimization of error calculation treating it as unknown. The value of T_C determined from that procedure (104.7 °C) was nearly identical to the value measured by DSC (105 °C), demonstrating the accuracy and the physical relevance to the cure onset temperature of vinyl hybrid. The results of the α_{max} model were compared to measured data, showing a difference of ~8% (Figure 5).

Using both models to predict the cure behavior of the vinyl hybrid resin, a cure cycle map was constructed to guide efforts to minimize cycle time. A code was written (MATLAB) to simulate different cure cycles and compare final degrees of cure. First, a final degree of cure, α_{max}, was determined using the expression for α_{max}, then input into the equation for the FC model. This equation was then employed to generate a final degree of cure for any specified cure cycle. The aspects of a cure cycle that were varied included temperature ramp rate, mid-stage hold time, mid-stage temperature, maximum temperature, and hold time at maximum temperature. The results were used to generate a 3D plot of final degree of cure as a function of one of the varied parameters and the total cure cycle time (Figure 6). In the plot, the red plane represents an α value of 0.99, and the purple plane includes possible combinations of T and t that meet or exceed that value.

The space visible above the red plane represents possible cure parameterization. To generate Figure 6,
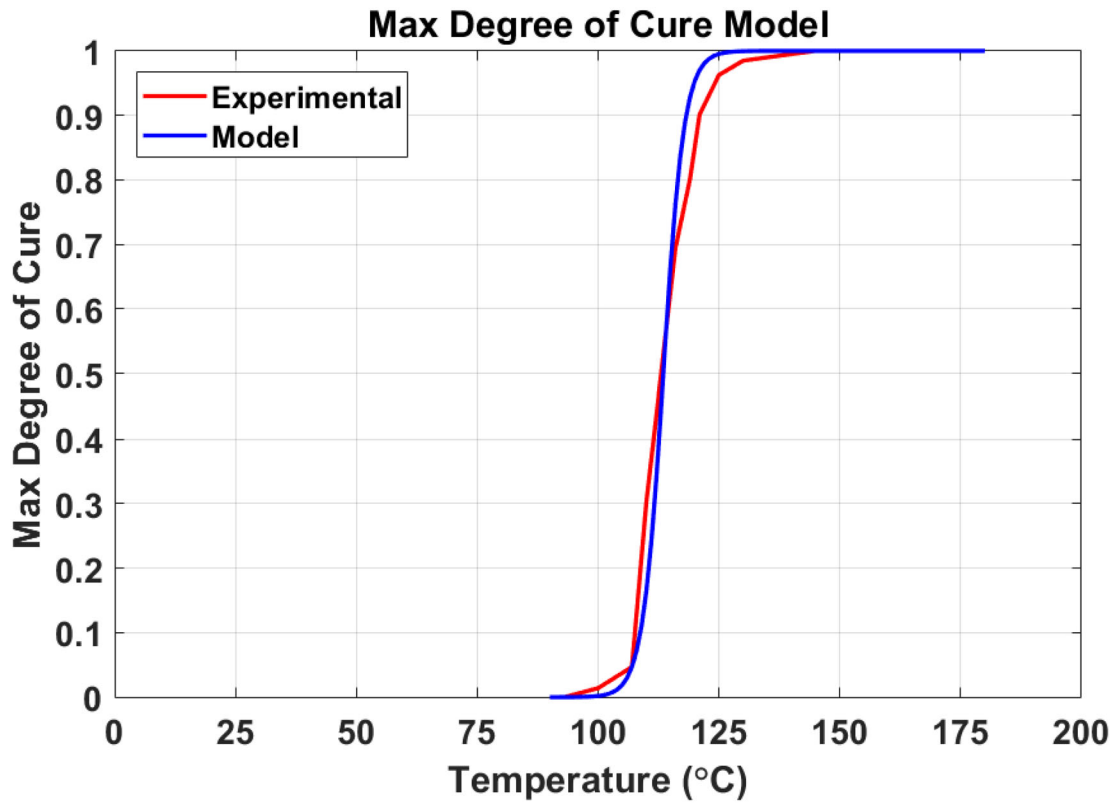
Figure 5. α_{max} as a function of maximum temperature.

a maximum temperature range of 110-170 °C was employed, using hold times at maximum temperature of 1-30 min. The ramp rate was 20 °C/min Through iterations of this process, one can design cure cycles of minimum duration that also achieve a final degree of cure of at least 0.99.

3.2. Model validation – sample cure cycles

To validate the model predictions and test the effects of varying aspects of the cure cycle, panels were fabricated using vinyl hybrid semi-preg. A control panel was cured using a five-hour cure cycle to produce a void-free laminate and provide a benchmark for mechanical performance. This cycle was the following: a single 30-minute debulk at 20 °C on the entire laminate, 60 min ramp to 90 °C, 30 min hold at 90 °C, 30-minute ramp to 150 °C, 60 min hold at 150 °C, and finally a 90-minute cool down to room temperature. In addition, panels were fabricated using five fast-cure cycles and compared against the control panel. The cure cycle parameters that were varied included maximum temperature, mid-stage hold time, and room temperature debulking time. Each sample was held at the maximum temperature for 10 min. Maximum temperatures were 150 °C or 120 °C to test the predictive accuracy of the FC model. The model predicted full cure ($\alpha = 1$) for 150 °C, and $\alpha = 0.17$ for 120 °C. A duration of 10 min was assigned to both the mid-stage hold at 90 °C and to room temperature debulking,

and the total ramp time to reach the final temperature was also 10 min. For cure cycles with a mid-stage hold, 5 min was assigned to each ramp before and after the hold. The test matrix of fabricated panels is shown in Figure 7.

As an example, the cure cycle for Panel 5 consisted of the following steps: 10 min debulk at room temperature, 5 min ramp to 90 °C, 10 min hold at 90 °C, 5 min ramp to 150 °C, 10 min hold at 150 °C, and finally a 10 min cool down to room temperature. After fabrication, the panels were then evaluated for quality and performance metrics.

The percent porosity of the panels (measured from polished sections) is shown in Figure 8a.

The porosity of the panels (Figure 8a) depended strongly on the room temperature debulk and mid-stage hold times. The control panel showed <0.1% porosity. Panels 2 and 5 included both steps and exhibited the lowest porosity among fast-cured samples (3.0% and 3.3% respectively). This finding is consistent with assertion that porosity depends strongly on the debulk and mid-stage hold, since both steps were included in the cure cycles for each panel. Sample 4 exhibited lower porosity than Sample 3, indicating that debulking had a greater effect on porosity reduction than a mid-stage hold when the steps were mutually independent. Sample 1 included neither step, and exhibited the highest porosity level.

The micrographs in Figure 8b highlight the differences in void characteristics between the different samples. The top sample is the control panel, and
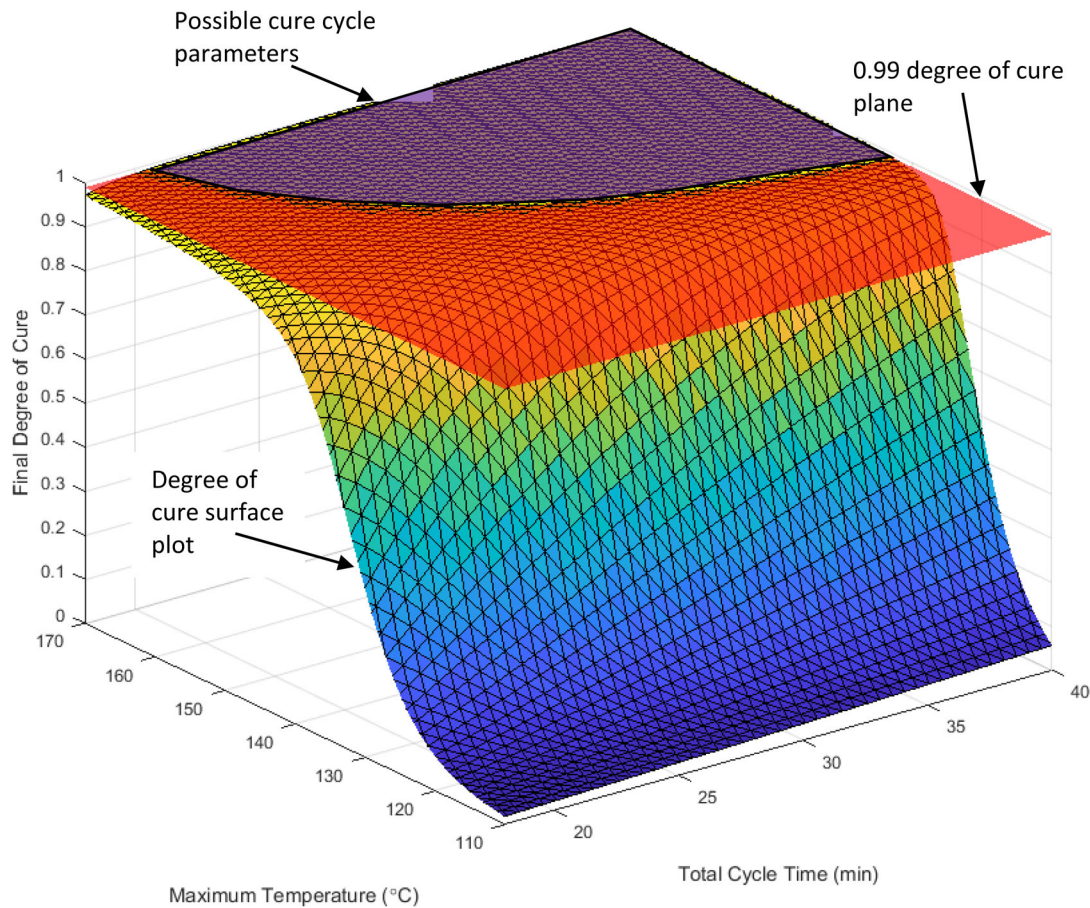
Figure 6. MATLAB simulation of cure cycle.

Figure 7. Sample test matrix.

showed negligible porosity, while the middle image is Panel 2 (3% porosity), and the bottom image is Panel 1 (6.5% porosity).

The porosity data indicate that both a mid-stage hold and a room-temperature debulk effectively reduce porosity, with debulking having a stronger effect. Panel 1 was fabricated without debulking or mid-stage hold, and exhibited both micro- and macro-voids. In Panel 2, interply voids stemming from air entrapment were prevalent, despite fabrication with both debulking and mid-stage hold steps. Similar voids were present in Panel 5, which was fabricated with the same cure cycle except for a different T_{max}. Unlike Panels 2 and 5, Panel 4 exhibited higher levels of interply porosity, despite fabrication with the same debulking time. However,

Panel 4 spent 5 min less time below 105 °C than Panel 5, which led to the higher macrovoid content. Panels 1 and 3, both of which did not have a debulking step, exhibited the most porosity. Although all panels exhibited porosity (except the control panel), increasing debulking time reduced porosity proportionately.

The measured values of T_g confirm model predictions for the degree of cure. Panel 2, which underwent the lower maximum temperature cycle, exhibited a lower T_g than other panels. The FC model predicted full cure versus incomplete cure when comparing two different cure temperatures, 120 °C and 150 °C, and a hold time of 10 min. Furthermore, other panels exhibited T_g values similar to the control panel, demonstrating that despite a cure time of 10 min, the panels reached full cure using a cycle designed using model predictions. Results for the short beam strength of the panels are shown in Figure 9.

Figure 9 shows interlaminar shear strength (ILSS) values for the 5 panels. The value for Panel 2 is not shown in Figure 9, because those panels were not fully cured, and thus exhibited lower strength values than other panels to the extent that an accurate measure was unable to be gathered. The trend in panel strength shows increasing ILS as panel number increases (and porosity decreases). Porosity
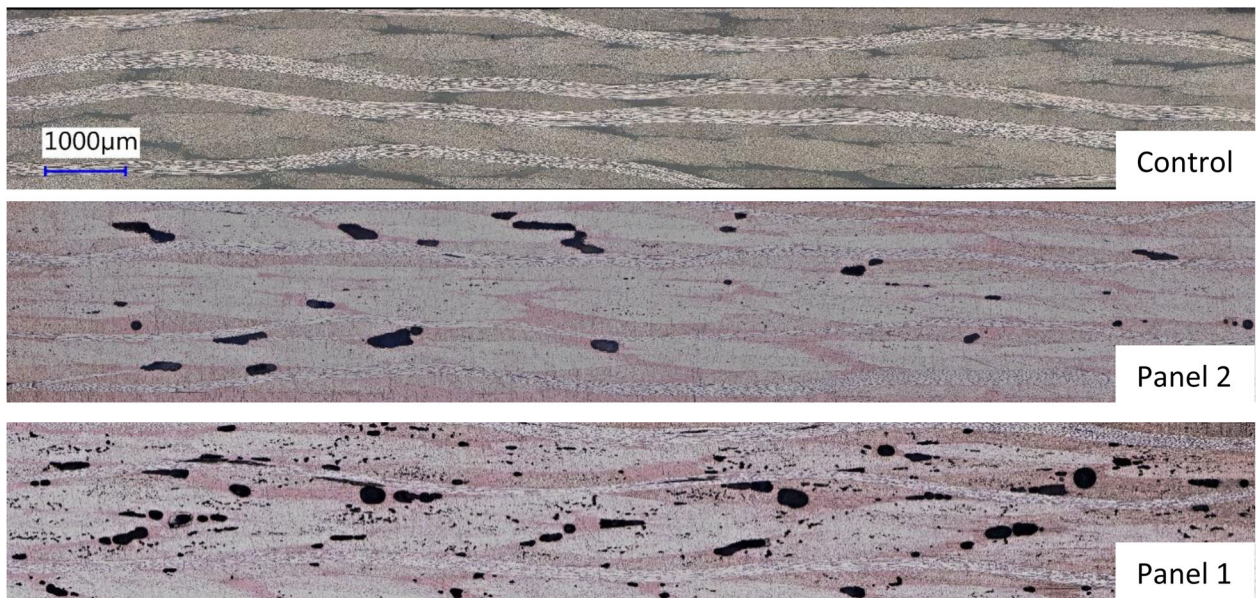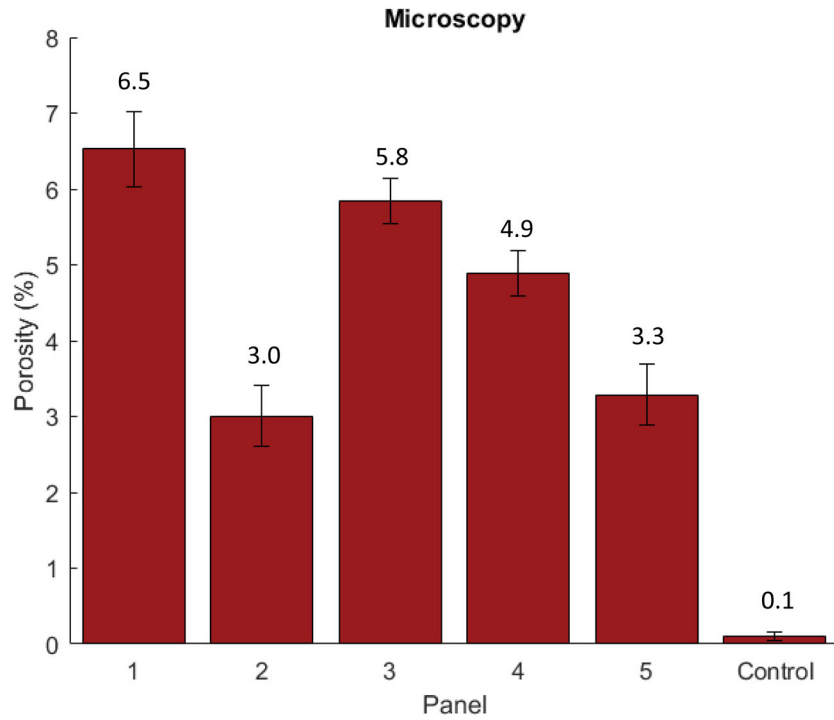
Figure 8. Porosity of fabricated panels **a)** percent porosity **b)** micrographs of panels.

reportedly decreased ILS, and the ILS values measured here exhibited similar dependence [26, 27]. The ILS for Panel 5, with the lowest porosity of the panels outside of the control, was >95% of the ILS of the control panel.

The ILS data demonstrate that with appropriate cure cycles and use of semi-preg formats to enhance air removal, fast-cure resins can be used with vacuum-bag cure to achieve mechanical performance similar autoclave cured prepregs. In addition, the revised FC model can be used to design an effective fast-cure cycle that achieves full cure. Although the ILS values for fast-cured panels were less than that

of the control panel, the difference was modest (< 5%), and was attributed to porosity within the panels. By reducing porosity and designing a suitable fast-cure cycle, panels with properties equivalent to a control panel can be achieved.

4. Conclusions

Fast-curing semi-pregs were modeled and evaluated using a vinyl hybrid resin. The conventional autocatalytic model was modified to account for peculiar features of the fast-cure resin (FC), particularly the inhibition of cure. This FC model was used to design
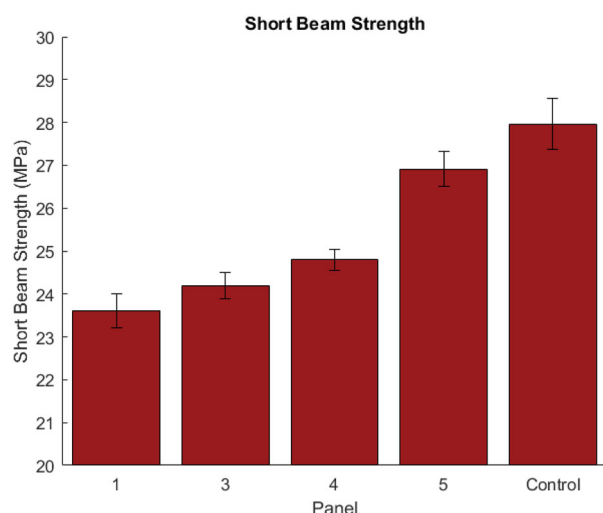
Figure 9. Interlaminar shear strength of panels.

cure cycles through prediction of kinetic behavior on a time scale of minutes. Panels were produced with short cure cycles (< 1 h) based on model calculations. Panels exhibited full cure and porosity levels of 1-7%. In principle, these porosity levels can be reduced by extending the debulk time and/or the mid-stage dwell, or using slower ramps to promote air evacuation during cure. Although there may always be tradeoffs between shorter cure cycles and part quality, inherent advantages of semi-preg will generally allow shorter cycle times when compared to conventional prepregs. Despite aerospace applications generally requiring the lowest porosity levels, shorter cure cycles without autoclaves will have clear benefits. Industries that produce in larger volumes (such as automotive) generally require shorter cycle times, but can often tolerate higher porosity levels. Further refinements to semi-preg format and resin formulation may be required to adapt to the needs of different industrial sectors.

The processability and room temperature stability of the vinyl hybrid resin are appealing features for applications beyond manufacturing of primary structures. One such application is repair of composite structures. Conventional repair materials and methods require specialized depots to perform repairs because of the limitations of employing conventional OoA prepregs. The room temperature stability of the vinyl hybrid obviates the need for cold storage of prepregs, an important attribute for in-field repairs. In addition, the relatively low cure temperature required and smaller exotherm of the vinyl hybrid resin (compared to epoxies) are features well-suited to repair of sensitive structures. The semi-preg format could potentially simplify the process for in-field repairs, reducing the need for expertise and specialized equipment.

In this work, two unconventional practices were combined and evaluated – fast-cure resin and VBO cure of semi-preg. The semi-preg format reduces the times required for debulking, hold and cure times, shrinking the process window for conventional materials from several hours to less than an hour. While these practices are mutually compatible, they can be deployed separately, also. When used with conventional thermosets (e.g. epoxies), the semi-preg format affords distinct advantages with respect to air removal during consolidation. Similarly, vinyl hybrid formulations can be used in conventional prepreg formats, offering both rapid cure characteristics and eliminating cold storage requirements. Nevertheless, the greatest benefits will accrue from deploying both technologies simultaneously. Doing so may ultimately enable expansion of composite materials into new markets and applications.

Acknowledgements

Disclosure statement

No potential conflict of interest was reported by the author(s).

ORCID

David B. Bender http://orcid.org/0000-0001-6503-6221
Steven Nutt http://orcid.org/0000-0001-9877-1978

References

[1] Helmus R, Kratz J, Potter K, et al. An experimental technique to characterize interply void formation in unidirectional prepregs. J Compos Mater. 2017;51(5):579–591.

[2] Gangloff JJ, Cender TA, Eskizeybek V, et al. Entrapment and venting of bubbles during vacuum bag prepreg processing. J Compos Mater. 2017; 51(19):2757–2768.

[3] Hubert P, Fernlund G, Poursartip A. Autoclave processing for composites. In Manuf. Tech. Polym. Matrix Compos. Elsevier, 2012. pp. 414–434.

[4] Upadhya AR, Dayananda GN, Kamalakannan GM, et al. Autoclaves for aerospace applications: issues and challenges. Int J Aerosp Eng. 2011;2011:1–11.

[5] Sherwin GR. Non-autoclave processing of advanced composite repairs. Int. J. Adhes. Adhes. 1999;19(2-3):155–159.

[6] Centea T, Grunenfelder LK, Nutt SR. A review of out-of-autoclave prepregs – Material properties, process phenomena, and manufacturing considerations. Compos Part A Appl Sci Manuf. 2015;70: 132–154.

[7] Koushyar H, Alavi-Soltani S, Minaie B, et al. Effects of variation in autoclave pressure, temperature, and vacuum-application time on porosity and mechanical properties of a carbon fiber/epoxy composite. J Compos Mater. 2012;46(16): 1985–2004.

[8] Cender TA, Simacek P, Advani DSG. Gas evacuation from partially saturated woven fiber preforms. Transp Porous Media. 2016;115:541–562.

[9] Kourkoutsaki T, Comas-Cardona S, Binetruy C, et al. The impact of air evacuation on the impregnation time of out-of-autoclave prepregs. Compos Part A Appl Sci Manuf. 2015;79:30–42.

[10] Centea T, Hubert P. Out-of-autoclave prepreg consolidation under deficient pressure conditions. J Compos Mater. 2014;48(16):2033–2045.

[11] Préau M, Hubert P. Processing of co-bonded scarf repairs: void reduction strategies and influence on strength recovery. Compos Part A Appl Sci Manuf. 2016;84:236–245.

[12] Hou TH, Jensen BJ. Double-vacuum-bag technology for volatile management in composite fabrication. Polym Compos. 2008;29(8):906–914.

[13] Archer E, McIlhagger A. Repair of damaged aerospace composite structures. Polym. Compos. Aerosp. Ind., Elsevier, 2015. pp. 393–412.

[14] Halley PJ, Mackay ME. Chemorheology of thermosets - an overview. Polym Eng Sci. 1996;36(5):593–609.

[15] Warnock CM, Briggs TM. Cure cycle development and qualification for thick-section composites. Int. SAMPE Tech. Conf. 2016-Janua 2016.

[16] Lukaszewicz DHJA, Ward C, Potter KD. The engineering aspects of automated prepreg layup: History, present and future. Compos Part B Eng. 2012;43(3):997–1009.

[17] Malnati P, Sloan J. Fast and Faster: Rapid-cure resins drive down cycle times, 2018. http://www.compositesworld.com/articles/fast-and-faster-rapid-cure-epoxies-drive-down-cycle-times.

[18] Mazza JJ, Storage KM. Bonded repair in the United States Air Force and work to expand future capability. STO-MP-AVT-266. 2018;1–22. http://doi.org/978-92-837-2172-7.

[19] Kamal MR, Sourour S. Kinetics and thermal characterization of thermoset cure. Polym Eng Sci. 1973;13(1):59–64.

[20] Cole KC. A new approach to modeling the cure kinetics of epoxy amine thermosetting resins. 1. Mathematical development. Macromolecules. 1991;24(11):3093–3097.

[21] Bernath A, Kärger L, Henning F. Accurate cure modeling for isothermal processing of fast curing epoxy resins. Polymers (Basel). 2016;8(11):319–390.

[22] Schechter SGK, Centea T, Nutt SR. Polymer film dewetting for fabrication of out-of-autoclave prepreg with high through-thickness permeability. Compos Part A Appl Sci Manuf. 2018;114:86–96.

[23] Malnati P. Hybrid resin system: Epoxy benefits, without the epoxy. Compos World. 2019. http://www.compositesworld.com/blog/post/hybrid-resin-system-epoxy-benefits-without-the-epoxy.

[24] Grunenfelder LK, Dills A, Centea T, et al. Effect of prepreg format on defect control in out-of-autoclave processing. Compos Part A Appl Sci Manuf. 2017;93:88–99.

[25] Khoun L, Centea T, Hubert P. Characterization methodology of thermoset resins for the processing of composite materials — case study: CYCOM 890RTM Epoxy Resin. J Compos Mater. 2010;44(11):1397–1415.

[26] Costa ML, Almeida SFM. d, Rezende MC. The influence of porosity on the interlaminar shear strength of carbon/epoxy and carbon/bismaleimide fabric laminates. Compos Sci Technol. 2001;61(14):2101–2108.

[27] Chamis CC, Handler LM, Manderscheid JM. Comp2007–002, 2019. 1–8.